Comb-Like Fluorinated Polystyrenes Having Different Side Chain Interconnecting Groups

Byoung Gak Kim,[†,‡] Jae-Seung Chung,[†] Eun-Ho Sohn,[†] Seung-Yeop Kwak,[‡] and Jong-Chan Lee*[,†]

Department of Chemical and Biological Engineering, and Department of Materials Science and Engineering, Seoul National University, Gwanak-Ro, Gwanak-Gu, Seoul 151-744, Korea

Received December 10, 2008; Revised Manuscript Received February 25, 2009

ABSTRACT: Comb-like fluorinated polystyrenes with different side chain interconnecting groups between backbone and side chain, such as ether (PST−O), thioether (PST−S) and sulfone (PST−SO_2), were synthesized in order to examine the effect of the interconnecting groups on the surface order and properties. Near edge X-ray absorption fine structure spectroscopy and grazing incidence wide-angle X-ray diffraction showed that PST−SO_2 with very polar sulfone groups exhibited a lower tilt angle of the fluorinated helix to the surface normal as well as higher packing density of fluorinated alkyl side chains than PST−O and PST−S, which have less polar groups. As a result of the ordered structure at the polymer-air interface, PST−SO_2 has a smaller surface energy and better stability in water than PST−O and PST−S. These results suggest that the introduction of polar groups to the side chains of comb-like fluorinated polymers can improve the surface properties including the hydrophobicity and stability of fluorinated surfaces.

Introduction

Comb-like fluorinated polymers are widely used in a variety of applications, such as coatings, electronics and medical materials, on account of their low surface energy.[1−6] The closely packed array structure of trifluoromethyl groups in the fluorinated side chains of comb-like polymers can lower the surface energy. In addition, the packing density of fluorinated alkyl side chains is influenced by the backbone and side chain structure of the comb-like fluorinated polymer.[7−12] For example, a comb-like fluorinated polymer with a flexible backbone structure has a lower surface energy than those with a rigid backbone because a more ordered structure of fluorinated side chains can be more easily formed through conformational changes of a more flexible backbone structure.[11,13−15] When the backbone structures of comb-like fluorinated polymers are identical, polymers with longer fluorinated side chains have lower surface energy because ordered side chain structures can be achieved more easily from the longer chains through side chain crystallization.[16] For example, poly(fluoroalkyl acrylate)s containing short fluorinated side chains (number of fluorocarbon <6) have a poorly ordered state and poor water repellency, whereas those with long alkyl side chains (number of fluorocarbon >7) contain hexagonally packed fluorinated side chains with low surface energy.

It is believed that the interconnecting groups between the backbone and fluorinated side chains also affect the surface properties of the polymers. However, there are very few reports on how the interconnecting groups affect the surface energy.[15] In this study, comb-like fluorinated polystyrenes were synthesized with different side chain interconnecting groups, such as ether, thioether and sulfone groups (Figure 1). The effect of the side chain interconnecting groups on the surface ordering behavior, including some bulk properties of these polymers, is discussed according to results of differential scanning calorimetry (DSC), X-ray scattering, near edge X-ray absorption fine structure (NEXAFS) and grazing incidence wide-angle X-ray diffraction (GIWAXD).

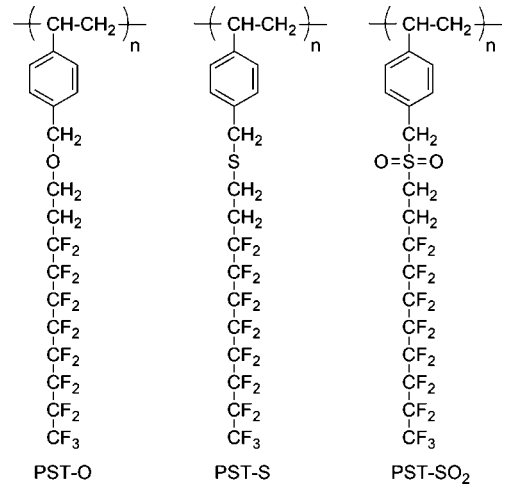

Figure 1. Chemical structure of the fluorinated polystyrenes.

Experimental Section

Materials. 2,2′-Azobis(isobutyronitrile) (Junsei) was recrystallized from methanol. *p*-Vinylbenzyl chloride (*p*-VBC, Aldrich), tetrabutylammonium hydrogen sulfate (TBAH, Aldrich), 1*H*,1*H*,2*H*,2*H*-perfluorinated decanol (Aldrich), 1*H*,1*H*,2*H*,2*H*-perfluorinated decanethiol (Aldrich), *m*-chloroperoxybenzoic acid (*m*-CPBA, Aldrich), and other solvents were used without further purification.

Synthesis. Poly[*p*-[[(perfluorooctylethylene)oxy]methyl]styrene] (PST−O) and poly[*p*-[[(perfluorooctylethylene)thio]methyl]styrene] (PST−S) were synthesized by free radical polymerization of fluorinated monomers in toluene as described in the literature.[17] Poly[*p*-[[(perfluorooctylethylene)sulfonyl]methyl]styrene] (PST−SO_2), was easily obtained by oxidation of PST−S with *m*-CPBA.

Preparation of *p*-[[(Perfluorooctylethylene)oxy]methyl]styrene. 1*H*,1*H*,2*H*,2*H*-Perfluorinated decanol (9.28 g, 20 mmol) and TBAH (0.7 g, 2 mmol) were mixed with an aqueous solution of 12 N NaOH (7.68 g in 16 mL) at 50 °C for 30 min, after which *p*-vinylbenzyl chloride (3.05 g, 20 mmol) was added. After 6 h, 20 mL of methylene chloride was added and the organic layer was

* Corresponding author. Telephone: +82-2-880-7070. Fax: +82-2-888-1604. E-mail address: jongchan@snu.ac.kr.
† Department of Chemical and Biological Engineering, Seoul National University.
‡ Department of Materials Science and Engineering, Seoul National University.

10.1021/ma8027535 CCC: $40.75
Published on Web 04/07/2009

washed with 0.5 N HCl and water. The crude product was purified by recrystallization from methanol, yielding white crystal. Yield: 65%. ^{1}H NMR ($CDCl_3$, δ in ppm): 2.44 (m, 2H), 3.76 (m, 2H), 4.53 (s, 2H), 5.27 (d, 1H), 5.78 (d, 1H), 6.71 (q, 1H), 7.30 (d, 2H), 7.40 (d, 2H).

Preparation of *p*-[[(Perfluorooctylethylene)thio]methyl]-styrene. 1*H*,1*H*,2*H*,2*H*-Perfluorinated decanethiol (9.68 g, 20 mmol) and TBAH (0.7 g, 2 mmol) were mixed with aqueous solution of 6 N NaOH (3.84 g in 16 mL) at room temperature for 30 min, after which *p*-vinylbenzyl chloride (3.05 g, 20 mmol) was added. After 6 h, 20 mL of methylene chloride was added and the organic layer was washed with 0.5 N HCl and water. The crude product was purified by recrystallization from methanol, yielding white crystal. Yield: 70%. ^{1}H NMR ($CDCl_3$, δ in ppm): 2.27 (m, 2H), 2.63 (m, 2H), 3.74 (s, 2H), 5.26 (d, 1H), 5.77 (d, 1H), 6.65 (q, 1H), 7.27 (d, 2H), 7.37 (d, 2H).

Preparation of Poly[*p*-[[(perfluorooctylethylene)oxy]methyl]-styrene] (PST−O). *p*-[[(Perfluorooctylethylene)oxy]methyl]-styrene (6.65 g, 12 mmol) was filled into a round-bottomed flask with AIBN (0.21 g, 1 mmol) and toluene (5.00 g, 54 mmol). After stirring at 60 °C for 12 h, the reaction mixture was poured into methanol, and the precipitate was purified by several reprecipitations from 1,1,2-trichlorotrifluoroethane into methanol. Yield: 75% ^{1}H NMR ($CDCl_3$/1,1,2-trichlorotrifluoroethane mixture, δ in ppm): 1.38 (2H), 1.71 (1H), 2.43 (2H), 3.73 (2H), 4.41 (2H), 6.50 (2H), 6.99 (2H). M_n = 15400, M_w = 26800.

Preparation of Poly[*p*-[[(perfluorooctylethylene)thio]methyl]styrene] (PST−S). This polymer was prepared from the same polymerization procedure as PST−O except that *p*-[[(perfluorooctylethylene)thio]methyl]styrene was used instead of *p*-[[(perfluorooctylethylene)oxy]methyl]styrene. Yield: 78% ^{1}H NMR ($CDCl_3$/1,1,2-trichlorotrifluoroethane mixture, δ in ppm): 1.38 (2H), 1.71 (1H), 2.34 (2H), 2.60 (2H), 3.65 (2H), 6.45 (2H), 6.97 (2H). M_n = 20300, M_w = 25100.

Preparation of Poly[*p*-[[(perfluorooctylethylene)sulfonyl]-methyl]styrene] (PST−SO_2). *m*-Chloroperoxybenzoic acid (0.74 g, 3.3 mmol) was added to a stirred solution of PST−S (0.90 g, 1.5 mmol) in chloroform/1,1,2-trichlorotrifluoroethane mixture (20 mL). After stirring at room temperature for 1 h, the reaction mixture was poured into methanol. After further extraction with methanol for 72 h using a Soxhlet extractor, the polymer was dried overnight in a vacuum oven. This product was obtained in 95% yield. ^{1}H NMR ($CDCl_3$/trifluoroacetic acid-*d*, δ in ppm): 1.00−1.40 (2H), 1.70−1.80 (1H), 2.69 (2H), 3.37 (2H), 4.40 (2H), 6.46 (2H), 7.00 (2H).

Analysis. The ^{1}H NMR spectra (300 MHz) were measured in either $CDCl_3$ or a $CDCl_3$/1,1,2-trichlorotrifluoroethane mixture using a JEOL JNM-LA 300 spectrometer. DSC was carried out on a TA Instruments 2920 differential scanning calorimeter at a heating rate of 5 °C /min. The melting transition temperatures were obtained at the maxima of the endothermic peaks, and the glass transition temperatures were taken as the point of inflection of the plot of the change in heat capacity with temperature in the DSC thermograms.

The molecular weights of PST−O and PST−S were determined by size exclusion chromatography in 1,1,2-trichlorotrifluoroethane at 30 °C using a Waters apparatus equipped with refractive index detection. Monodisperse poly(dimethylsiloxane)s were used as standards. In the case of PST−SO_2, the molecular weight could not be measured by GPC due to its insolubility in 1,1,2-trichlorotrifluoroethane. As described above, PST−SO_2 was obtained by the oxidation of PST−S. The molecular weight of PST−SO_2 is expected to be similar to or higher than that of PST−S. This is because the oxidation of thioether (−S−) to sulfone (−SO_2−) groups in the side chain of the polymers using *m*-chloroperoxybenzoic acid as the oxidation agent at mild condition (room temperature) does not decrease the molecular weights or cleave the polymer backbone.[18,19] Calculated number average molecular weight by considering a constant degree of polymerization after oxidation reaction is 21400 g/mol.

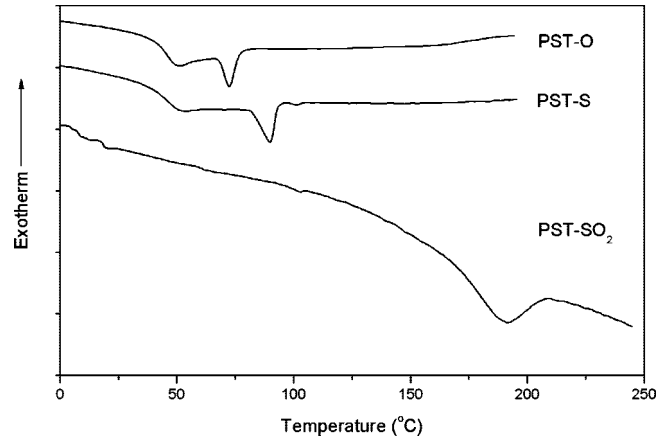

Figure 2. DSC curves of the fluorinated polystyrenes.

X-ray scattering measurements were carried out in transmission mode using synchrotron radiation at the 3C2 X-ray beamline at Pohang Accelerator Laboratory, Korea.

Two-dimensional grazing incidence wide-angle X-ray diffraction (GIWAXD) images were measured using a high-power X-ray beam (photon flux $\cong 10^{11}$ photons s^{-1} $mrad^{-1}$ per 0.1%, beam size $\leq$0.5 mm^2) from a synchrotron radiation source (4C2 beamline, Pohang Accelerator Laboratory, Korea) at λ = 1.3807 Å. The detection system equipped with a two-dimensional X-ray detector (PI-SCX4300−165/2, Princeton Instrument). Details of the analytical methodology has been reported elsewhere.[20,21]

Near edge X-ray absorption of fine structure (NEXAFS) experiments were carried out on the photoemission spectroscopy 2B1 beamline (beam size = 1 × 3 mm^2) at the Pohang Accelerator Laboratory, Korea. The C K-edge NEXAFS spectra were recorded in partial-electron-yield (PEY) mode. The soft X-ray incident angle was varied from 20 to 90° for polarization dependence. The PEY signals were normalized by the incident beam intensity obtained from the photo yield of a clean silicon surface.

The contact angles were determined using a Krüss DSA10 contact angle analyzer interfaced to drop shape analysis software. Both the advancing and receding angles were measured for drops of several solvents. The contact angles for each sample were measured more than four times on films independently prepared, and the average value was used. The contact angle variability was <1°.

Thin films of the polymer were prepared by spin-coating a 2 wt% solution of the polymer in 3,5-bis(trifluoromethyl)phenol onto a silicon wafer using a Laurell model WS-400A-6NPP/LITE spin-coater at 1000 rpm for 5 min. The films were dried in a vacuum oven for 72 h at room temperature, and annealed for 2 h at approximately onset point of the liquid crystalline melting temperature (40, 50, and 150 °C for PST−O, PST−S, and PST−SO_2, respectively). The estimated film thickness ranged from 20 to 40 nm according to atomic force microscopy (AFM, SPA300HV multifunction unit/SPI3800 probe station, Seiko Instruments Inc., Japan). The AFM images were obtained in tapping mode in air using a 20 μm × 20 μm scanner. The stylus surface roughness, R_a, of the thin films ranged from 0.7 to 1.9 nm.

Results and Discussion

Bulk Properties of Comb-Like Fluorinated Polystyrenes. Figure 2 shows the DSC traces of the fluorinated polystyrenes obtained at a heating rate of 5 °C/min. The endothermic transitions observed at 72.8, 99.9, and 186.7 °C for PST−O, PST−S and PST−SO_2 were found to be the liquid crystalline melting temperatures from the X-ray studies at elevated temperatures. Above the endothermic transition temperatures, the ordered peaks observed by XRD at room

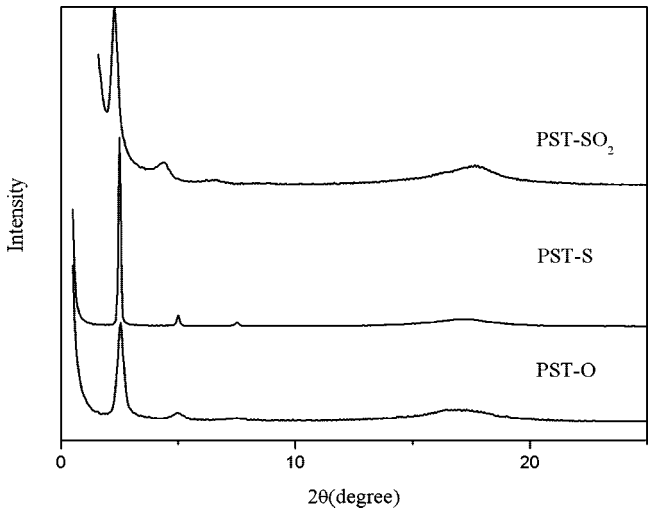

Figure 3. Powder X-ray diffraction patterns of the fluorinated polystyrenes.

Table 1. Thermal Properties of the Fluorinated Polystyrenes

	T_g (°C)	Transition, °C (ΔH, mJ/mol)
PST−O	44.1	72.8 (6.4)
PST−S	59.0	99.9 (9.6)
PST−SO_2		186.7 (37.9)

temperature disappeared. The glass transition temperatures (T_g) can be seen clearly from the DSC curves of PST−O and PST−S with melting transitions showing smaller values of enthalpy change (ΔH), while PST−SO_2 only showed a melting transition with a larger ΔH value (Table 1). We tried to observe the glass transition temperature of PST−SO_2 by quenching the melted samples into liquid nitrogen, however T_g was not observed. Shimizu et al. reported that comb-like fluorinated polyacrylates with longer fluoroalkyl side groups have highly ordered side chain structures (larger ΔH values) and show only melting temperatures (T_m) from DSC.[22] On the other hand, comb-like fluorinated polyacrylates with shorter fluoroalkyl side groups have poorly ordered side chain structures (smaller ΔH values) and show both T_g and melting temperature (T_m). PST−SO_2, which showed only the T_m, had a more ordered side chain structure than PST−O and PST−S, which showed both T_g and T_m from XRD, GIWAXD, and NEXAFS studies discussed in the later part of this paper. The T_g of PST−S was larger than that of PST−O, and the T_m values increase in the order of PST−O < PST−S < PST−SO_2. Therefore, it is expected that among the three polymers, the molecular interaction in PST−SO_2 is largest, and that in PST−O is smallest. This concurs with the order of the dipole moments of the oxide, thioether, and sulfone groups. For example, the dipole moments of dimethyl oxide, dimethyl thioether, and dimethyl sulfone are 1.30, 1.55, and 4.49 D, respectively.[23]

Figure 3shows the X-ray scattering curves of powder samples of fluorinated polystyrenes at 30 °C. A series of ordered reflections corresponding to the 001, 002, and 003 indices of a periodic layer suggest that fluorinated polystyrenes have the ordered structure. The *d*-spacing of the 001 reflection was approximately double that of the expected side chain length assuming that the side chains are fully extended with the trans conformations. Therefore, the fluorinated polystyrenes essentially have double-layered lamellar structures, while the layer distance increases in the order of PST−O (34.6 Å), PST−S (35.3 Å) and PST−SO_2 (38.4 Å). Considering the average bond lengths (C−O = 1.42 Å, C−S for thioether = 1.82 Å, and C−S for sulfone = 1. 77 Å) and angles (∠COC = 112°, ∠CSC for thioether = 99.1°, and ∠CSC for sulfone = 121°), the longer layer distance of PST−S (approximately 0.7 Å) than PST−O might be an intrinsic property, while the longest layer distance of PST−SO_2 has other causes.[23] On the other hand, the *d*-spacing of the wide-angle reflection representing the distance between the fluorinated alkyl side chains of PST−SO_2 is 5.0 Å, which is smaller than those of PST−O (5.2 Å) and PST−S (5.1 Å). The *d*-spacing of hexagonally packed fluorinated alkyl side chains is 5.0 Å as has been observed in poly(1*H*,1*H*,2*H*,2*H*-perfluordecyl acrylate) and fluoromethacrylate blockcopolymers with highly ordered fluorinated alkyl side chains.[8,11,15,24] To quantify the packing density of fluorinated alkyl side chains, correlation length was also determined from fwhm of peak at wide angle region, and they were found to be 26.9, 29.1, and 30.0 Å for PST−O, PST−S, and PST−SO_2, respectively. This indicates that PST−SO_2 with polar interconnecting sulfone groups has higher packing density of fluorinated alkyl side chains than PST−O and PST−S. This side chain structure possibly induces highly ordered lamellar structures with the largest layer distances, while PST−O and PST−S with less polar interconnecting ether groups contains more loosely packed (larger *d*-spacing) fluorinated alkyl side chains, which decrease the layer distance of the lamellar structures.[12,18,25,26] The slightly longer layer distance of PST−S than that of PST−O may be caused by the longer C−S bond length and/or smaller distance of fluorinated alkyl side chains.

Surface Order of Polymer Thin Films. The effect of the side chain interconnecting groups on the surface ordering of thin films of fluorinated polystyrenes was examined by GIWAXD and NEXAFS. Figure 4 shows the 2-dimensional GIWAXD maps of the fluorinated polystyrenes recorded at an incidence angle of $\alpha_i = 0.17°$. All the fluorinated polystyrenes showed three or four strong signals along the out of plane corresponding to the 001, 002, and 003 (001, 002, 003, and 004 for PST−SO_2) indices of the periodic lamellar layers and the one in-plane order signal corresponding to the packing distance of fluorinated alkyl side chains. A clear powder ring observed in the small angle regime (first order signal) from PST−SO_2 in Figure 4c indicates that the ordering of lamellar structure in PST−SO_2 might not be as good as those in PST−O and PST−S. Still the perfluorinated alkyl chains of PST−SO_2 on the surface have the highest degree of surface ordering and this gives lowest surface energy to PST−SO_2 as explained in the later part of this manuscript. Table 2 lists the *d*-spacings obtained from the 2-dimensional GIWAXD maps. The distances between the fluorinated alkyl side chains on the surface were almost identical to those in the bulk states for all fluorinated polystyrenes. On the other hand, the distances of lamellar layers on the surface were approximately 4 Å smaller than those in the bulk states. The lower *d*-spacing in the thin film indicates that the fluorinated alkyl side chains were tilted in the thin film as reported by Gruner et al.[20] The tilt in thin film is induced by the surface-induced tilt in the topmost smectic layer. The fluorinated tilt at the surface is propagated throughout the thin film. We also found that the fluorinated alkyl side chains of fluorinated polystyrenes are tilted from NEXAFS studies shown in the next part of this paper.

To quantify the in-plane ordering of fluorinated alkyl side chains, we also examined radial dependence of scattering intensity for scattering vectors q at an angle of $1° < \phi_d$ (azimutal angle) $< 5°$.[20] Correlation lengths ($2/\Delta q$) of PST−O, PST−S, and PST−SO_2 determined from fwhm are 7.66, 7.89, and 8.41 Å, respectively. This indicates that PST−SO_2 has higher packing density of fluorinated alkyl side chains at the surface than PST−O and PST−S.

The alignment of the fluorinated alkyl groups on the polymer surface was characterized further by NEXAFS analysis. NEXAFS is a very useful technique for determining the molecular

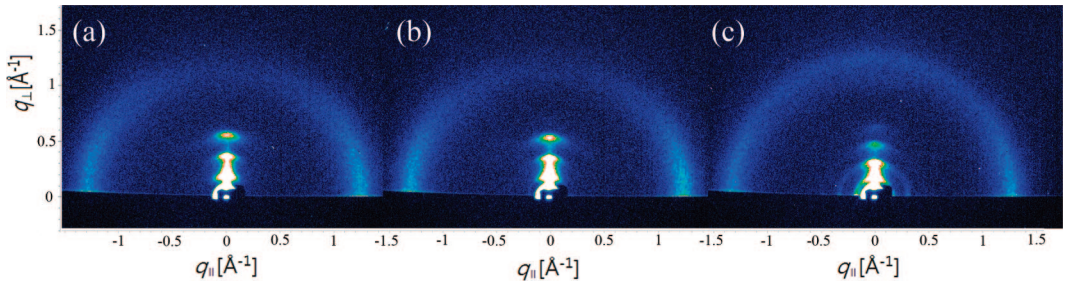

Figure 4. GIWAXD patterns of (a) PST−O, (b) PST−S, and (c) PST−SO_2 films.

Table 2. Powder WAXD, GIWAXD, and NEXAFS results of the fluorinated polystyrenes

	d-spacing (Å) from powder WAXD		*d*-spacing (Å) from GIWAXD		NEXAFS results		
	Small angle	Wide angle	Small angle[a]	Wide angle[b]	S_{C-F}[c]	$S_{F\text{-helix}}$[d]	$\tau_{F\text{-helix}}$ (deg)[e]
PST−O	34.6, 17.6, 11.8	5.2	31.0, 16.3,-10.9	5.2	−0.112	0.224	45.9
PST−S	35.3, 17.7, 11.8	5.1	32.3, 17.2,-11.4	5.1	−0.136	0.272	44.2
PST−SO_2	38.4, 20.1, 13.5	5.0	33.6, 19.3, 12.8, 9.6	5.0	−0.207	0.414	38.7

[a] A series of *d*-spacings corresponding to the 001, 002, and 003 indices of a periodic smectic layer. [b] *d*-spacings representing the distance between the fluorinated alkyl side chains. [c] Surface orientational parameter of C−F bonds. [d] Surface orientational parameter of fluoroalkyl helix. [e] Tilt angle of fluoroalkyl helix to the surface normal.

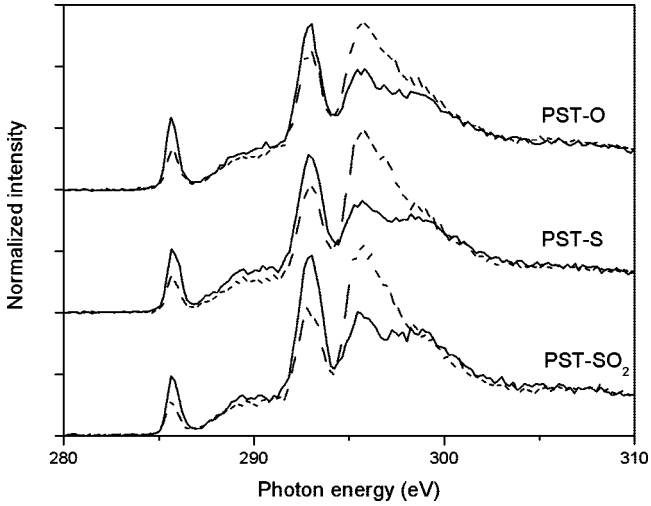

Figure 5. NEXAFS spectra of the C K edge of polymer thin films recorded at 90° (solid line) and 20° (dashed line).

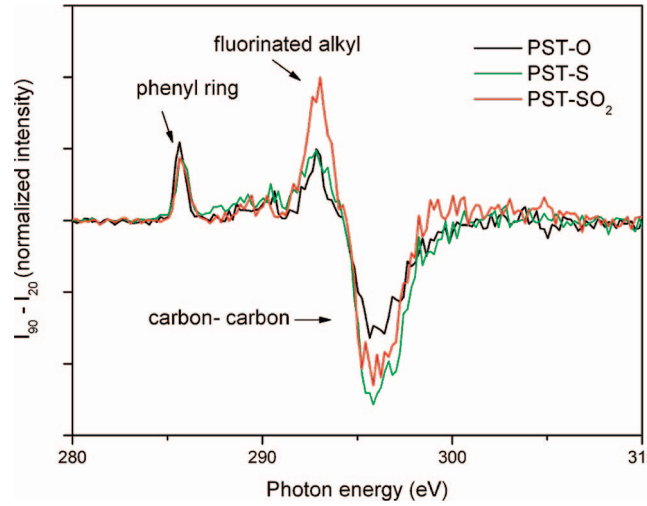

Figure 6. Difference NEXAFS spectra of the normalized C 1S edge of polymer thin films recorded at 90° and 20° ($I_{90} - I_{20}$).

orientation near the outermost surface. Details of this technique are reported elsewhere.[27−31] Figure 5 shows the NEXAFS spectra of the C1s edge of polymer thin films. There are four dominant peaks showing polarization dependence. The peak at 285 eV was assigned to excitation of the C 1s core electrons to the π^* (1s − π^*) of the carbon double bonds in the phenyl rings of the polymers. A sharp peak at approximately 292 eV and smaller peaks at 296 eV were assigned to the 1s−σ^* transition for the C−F and C−C bonds, respectively. Small peak at approximately 288 eV can be assigned to the 1s−σ^* transition for C−H.[31] Figure 6 shows the polarization dependence (intensity recorded at 90° (I_{90}) − intensity recorded at 20° (I_{20})) of the fluorinated polystyrenes. For all polymers, the peak intensity of the C−F bonds at 90° (normal incidence) was larger than that at 20° (grazing incidence). In contrast, the C−C bond peak had a larger intensity from the grazing incidence than that from the normal incidence. This suggests that the fluorinated alkyl side chains of the fluorinated polystyrenes are oriented near-perpendicular to the film surface. Comparing the linear dichroism (intensity difference) of C−F bonds, one could notice that PST−SO_2 has the highest degree of ordering of fluorinated alkyl side chains on the surface. Therefore, the polar sulfone groups in the side chain can improve the ordering of fluorinated alkyl chains on the surface. The peak intensity of the C═C bonds at 90° (normal incidence) was larger than that at 20° (grazing incidence) indicating that the phenyl ring of the fluorinated polystyrenes are aligned perpendicularly to the surface normal, while the intensity differences of the two peaks are almost identical for all cases. This suggests that the orientation of phenyl groups is unaffected by the introduction of different side chain interconnecting groups.

Tilt angles of rigid fluoroalkyl side chains was estimated from the order parameters (C−F bond) calculated from the peak intensities of the C−F bonds at a grazing incidence angle and normal incidence angle (Table 2).[32] The order parameter values of the fluoroalkyl helices increased again in the order of PST−O, PST−S, and PST−SO_2. The tilt angle of the fluoroalkyl helix of PST−O, PST−S, and PST−SO_2 was approximately 45.9, 44.2, and 38.7° with the surface normal, respectively. Therefore, among the three polymers, the perfluorinated alkyl chains of PST−SO_2 on the surface have the highest degree of surface ordering.

Surface Energies and Reconstruction of Polymer Thin Films. Table 3 shows the surface roughness and advancing contact angles for the various test solvents of the polymer thin films. The surface roughness, R_a, obtained by AFM ranged of 0.7 to 1.9 nm. Since the R_a values of the polymers are quite

Table 3. Surface Roughness and Advancing Contact Angles of the Fluorinated Polystyrene Films

		advancing contact angle (deg)								
	R_a (nm)	water	FA[b]	DIM[c]	EG[d]	BA[e]	octane	decane	Dodecane	Hexadecane
PST−O	1.9	123.6	[a]	102.7	105.5	91.7	66.8	71.8	74.9	79.1
PST−S	1.7	122.8	[a]	101.8	102.6	91.2	67.3	72.2	75.5	79.2
PST−SO_2	0.7	126.1	109	105.1	104.3	92.0	67.9	72.7	75.7	79.2

[a] Polymer films were partially soluble in formamide. [b] Formamide. [c] Diiodomethane. [d] Ethylene glycol. [e] Benzyl alcohol.

Table 4. Surface Energy (Acid−Base Theory) of the Fluorinated Polystyrene Films

	PST−O			PST−S			PST−SO_2		
	γ^{LW}	$\gamma^{acid-base}$[a]	γ^{total}	γ^{LW}	$\gamma^{acid-base}$	γ^{total}	γ^{LW}	$\gamma^{acid-base}$	γ^{total}
water−DIM[b]−EG[c]	7.73	0.21	7.94	8.04	0.20	8.24	6.95	−0.06	6.89
water−DIM−BA[d]	9.16	0.09	9.24	9.43	0.11	9.54	8.57	0.03	8.61
water−DIM−octane	8.51	0.14	8.65	8.71	0.17	8.87	7.86	0.07	7.93
water−BA−octane	11.3	0.01	11.3	11.3	0.02	11.4	11.1	0.01	11.1
water−EG−octane	10.5	−0.02	10.5	10.4	0.05	10.4	10.2	−0.05	10.2
DIM−EG−octane	8.51	0.18	8.70	8.71	0.44	9.14	7.86	0.47	8.33
DIM−EG−BA	9.16	0.09	9.24	9.43	0.26	9.69	8.57	0.28	8.85

[a] $\gamma^{acid-base} = 2(\gamma^{acid}\ \gamma^{base})^{1/2}$. [b] Diiodomethane. [c] Ethylene glycol. [d] Benzyl alcohol.

small, the influence of surface roughness on the contact angle can be ignored in all contact angle measurements; a smooth surface (R_a < 100 nm) does not affect the contact angle of polymer films.[33] The advancing contact angles of PST−SO_2 were larger than those of PST−O or PST−S for most solvents used in the contact angle measurement. The contact angles of PST−O and PST−S films could not be measured using formamide because they are partially soluble in formamide, while PST−SO_2 film is insoluble with a contact angle of 109°. The contact angle and film stability are another strong indication that the CF_3 moieties (end group of the fluorinated alkyl side chain) of PST−SO_2 are well exposed on the outmost surface to prevent interactions between the probing liquids and nonfluorinated comparably polar regions of the polymer, such the styrene backbones and side chain connecting groups. The surface energy of the fluorinated polystyrenes was obtained by applying the advancing contact angle results to surface tension component theory (acid−base (van Oss) approach)). It has been suggested that the acid−base (van Oss) approach is a generalization of the Fowkes approach, by considering the perceived acid−base interactions at the interface.[34] The surface tension was divided into different perceived components, Lifshitz-van der Waals (γ^{LW}), acid (γ^+), and base (γ^-) components, such that the total surface tension can be given by the following equation:

$$\gamma_i = \gamma_i^{LW} + 2(\gamma_i^+\gamma_i^-)^{1/2} \quad (1)$$

Here *i* denotes either the solid or liquid phase. The interfacial tension was postulated from both solid−liquid or liquid−liquid systems as follows:

$$\gamma_{12} = \gamma_1 + \gamma_2 - 2(\gamma_1^{LW}\gamma_2^{LW})^{1/2} - 2(\gamma_1^+\gamma_2^-)^{1/2} - 2(\gamma_1^-\gamma_2^+)^{1/2} \quad (2)$$

For a solid−liquid system, combining eq 2 with Young's equation yields the following:

$$\gamma_l(1+\cos\theta) = 2(\gamma_l^{LW}\gamma_s^{LW})^{1/2} + 2(\gamma_l^+\gamma_s^-)^{1/2} + 2(\gamma_l^-\gamma_s^+)^{1/2} \quad (3)$$

where θ is the advancing contact angle. Since this equation contains three unknowns (γ_s^{LW}, γ_s^+ and γ_s^-) of the solids, it has been recommended for measuring the contact angles using more than three different liquids. Table 4 shows the total surface energy and surface energy component of the fluorinated polystyrenes obtained using this approach. The surface energies of PST−SO_2 were lowest among the three fluorinated polystyrenes in all case, while it varied from 6.89 to 11.08 mJ/m^2 according to different solvent systems used. This can be explained by environmental-dependent surface reconstruction.

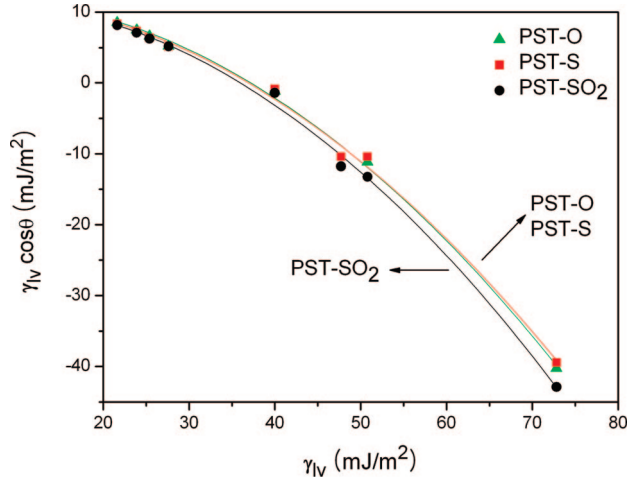

Figure 7. γ_{lv} vs $\gamma_{lv}\cos\theta$ for the contact angle data on the fluorinated polystyrenes thin films.

Because of surface reconstruction, the surface composition is expected to be different for each probe liquid, depending on polarity of the liquid.[35,36] However, the value of γ_{sv} is assumed to be constant regardless of the solvent system since the surface energy of a solid (γ_{sv}) is a thermodynamic property of the solid. Therefore, inconsistency of the surface energy suggests that the calculation of the surface energy using this approach is flawed.[37] In an effort to estimate intrinsic surface energy of a solid, Kwok and Neumann derived an expression relating the contact angle of a solid to γ_{lv} and γ_{sv} using eq 4. Only one constant surface energy value can be obtained because this approach is based on the equation of state relating γ_{lv} and γ_{sv} and a series of solvents with different surface tensions.

$$\cos\theta = -1 + 2(\gamma_{sv}/\gamma_{lv})^{1/2}(1 - \beta_1(\gamma_{lv} - \gamma_{sv})^2) \quad (4)$$

The surface energy of the fluorinated polystyrenes was estimated using this equation of state approach from 8 types of solvents ranging from water with the largest surface tension to octane with the lowest surface tension. The curves shown in the Figure 7 are best-fits of eq 4 to the experimental data of γ_{lv} and θ. Table 5 shows the surface tension (γ_{sv}) and constant (β_1) of the fluorinated polystyrene thin films determined using a two-variable (γ_{sv}, β_1) least-squares fit. Some contact angle data are not included to derive the curves if they deviate too much.[34] In this case, the ethylene glycol data of PST−O was not included. Using this approach, PST−SO_2 had lowest surface energy, and

Table 5. Surface Energy (Equation of State Approach) of the Fluorinated Polystyrene Films

	γ_{sv}[a]	$\beta_1 \times 10^{4}$[b]	R^{2}[c]
PST−O	10.88	1.085	0.9987
PST−S	10.71	1.031	0.9960
PST−SO_2	10.56	1.194	0.9970

[a] Surface tension. [b] Constant depending on the material. [c] Relation constant.

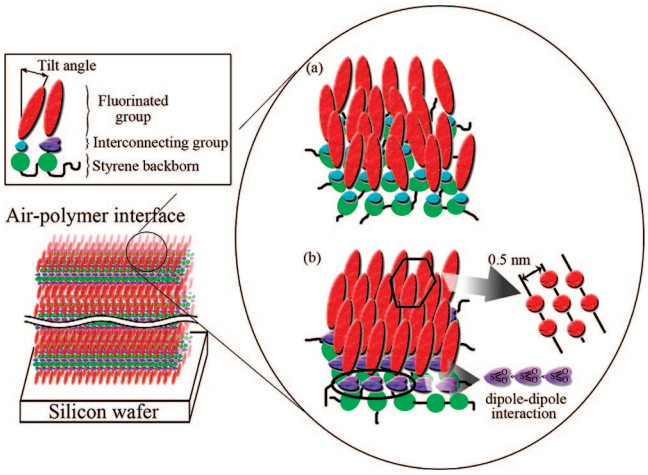

Figure 8. Schematic diagram of the surface order of the fluorinated polystyrenes with side chain (a) (thio)ether linkage and (b) sulfone linkage.

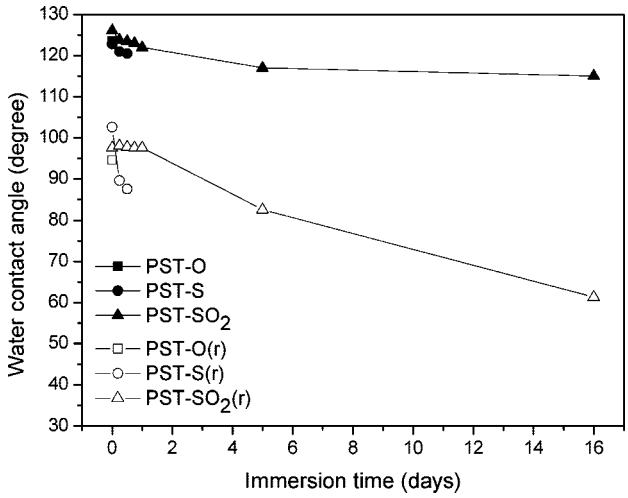

Figure 9. Time dependence of the advancing and receding water contact angles of fluorinated polystyrene films on immersion in water.

the surface energy of PST−S was slightly lower than that of PST−O. This result is consistent with the other results reported in this paper. Both the bulk and surface properties showed that PST−SO_2 has the highest ordering of lamellar and fluorinated alkyl side groups, and PST−S and PST−O have similar levels of ordering, even though PST−S appears to have a slightly higher ordered structure. From these results, a schematic diagram was produced to show the surface structures of well ordered PST−SO_2 with strongly polar interconnecting sulfone groups and less ordered PST−S and PST−O with less polar ether and thioether groups. (Figure 8)

The contact angle change was measured as a function of the immersion time of the polymer films in water over a 16 day period to determine the film stability (Figure 9). The hydrophobic surface properties of PST−O and PST−S were lost within 1 day in the polar environment (water). For example, receding contact angle of PST−S decreased sharply by 16° after 1 day immersion in water and dynamic contact angle measurement on PST−O and PST−S surface film immersed in water for more than 2 days was not possible possibly due to the surface reconstruction as reported from other fluorinated polymers.[8] In contrast, the PST−SO_2 film maintained its shape and structure for more than 16 days even though both the advancing and receding contact angles of the PST−SO_2 film had decreased over the 16 day period. A decrease in contact angle of 10° over a 16 day period means that the surface of the PST−SO_2 film reconstructs to some degree in water, while not much. Therefore the outmost surface of the PST−SO_2 film is still dominated by fluorocarbon parts, even after 16 days in water. Others reported that the surfaces of side-chain liquid crystalline fluorinated polymers with nonpolar linkage such as ether or ester coated the surface treated glass were unaffected even after 2 weeks of immersion in water or seawater.[31,38] We believe that if we had treated the surfaces of the substrate (silicon wafer) properly using organic silane compounds and polymer compatibilizers for the increase of the adhesion property, the surface stability of PST−O and PST−S films might be improved. In the case of PST−SO_2, the very hydrophobic surface property in water was maintained even on the untreated surface due to the dipole−dipole interactions between the sulfone groups which can prevent the reconstruction of fluorinated alkyl groups at the surface.

Conclusion

Comb-like fluorinated polystyrenes with different side chain interconnecting groups, such as ether (PST−O), thioether (PST−S), and sulfone (PST−SO_2), were synthesized and characterized. PST−SO_2 with very polar sulfone interconnecting groups showed much higher degree of order of both the bulk and surface structures than PST−O and PST−S, which have less polar thioether and ether groups, respectively. In particular, the fluorinated alkyl side groups of PST−SO_2 on the surfaces have a densely packed hexagonal structure with a shorter inter chain distance of approximately 5 Å, while PST−O and PST−S have more loosely packed (larger *d*-spacing) fluorinated alkyl side chains. As a consequence, PST−SO_2 has a lower surface energy and much better stability in water than PST−O and PST−S. The surface energy of PST−S was slightly lower than that of PST−O. This is possibly because the thioether groups is slightly more polar than the ether group, which gives the fluorinated alkyl side groups containing thioether groups a slightly better packing structure than those with ether groups. Therefore, the hydrophobicity and the stability of the fluorinated surfaces can be improved by introducing polar sulfone groups to the side chains of comb-like fluorinated polymers.

Acknowledgment. The authors thank the Korea Research Foundation through the Basic Research Program (Grant No. KRF-2008-314-D00112) and Ministry of Land, Transport, and Maritime Affairs for financial support. Experiments at PAL were supported in part by MEST and POSTECH.

References and Notes

(1) Hougham, G. In *Fluoropolymers*; Hougham, G., et al., Eds.; Plenum Press: New York, 1999.
(2) Scheirs, J., Ed. *Modern Fluoropolymers: High Performance Polymers for Diverse Applications*; Wiley: New York, 1997.
(3) Schmidt, D. L.; Coburn, C. E.; Dekoven, B. M.; Potter, G. E.; Meyers, G. F.; Fisher, D. A. *Nature (London)* **1994**, *368*, 39.
(4) Thorpe, A. A.; Peters, V.; Smith, J. R.; Nevell, T. G.; Tsibouklis, J. *J. Fluorine Chem.* **2000**, *104*, 37.
(5) Bryan-Brown, G. P.; Wood, E. L.; Sage, I. C.; Sage, I. C. *Nature (London)* **1999**, *399*, 338.
(6) Ober, C. K.; Gabor, A. H.; Gallagher-Wetmore, P.; Allen, R. D. *Adv. Mater.* **1997**, *9*, 1039.
(7) Genzer, J.; Efimenko, K. *Science* **2000**, *290*, 2130.

(8) Wang, J.; Mao, G.; Ober, C. K.; Kramer, E. J. *Macromolecules* **1997**, *30*, 1906.
(9) Park, I. J.; Lee, S. B.; Choi, C. K. *Macromolecules* **1998**, *31*, 7555.
(10) Thünemann, A. F.; Schnöller, U.; Nuyken, O.; Voit, B. *Macromolecules* **2000**, *33*, 5665.
(11) Kim, B. G.; Sohn, E. H.; Cho, K. W.; Lee, J.-C. *Eur. Polym. J.* **2008**, *44*, 2911.
(12) Kim, B. G.; Sohn, E. H.; Lee, J.-C. *Macromol. Chem. Phys.* **2007**, *208*, 1011.
(13) Tsibouklis, J.; Nevell, T. G. *Adv. Mater.* **2003**, *15*, 647.
(14) Owen, M. J. *Comments Inorg. Chem.* **1988**, *7*, 195.
(15) Corpart, J. M.; Girault, S.; Juhue, D. *Langmuir* **2001**, *17*, 7237.
(16) Honda, K.; Morita, M.; Otsuka, H.; Takahara, A. *Macromolecules* **2005**, *38*, 5699.
(17) Hopken, J.; Möller, M. *Macromolecules* **1992**, *25*, 1461.
(18) Kim, B. G.; Moon, J. K.; Sohn, E. H.; Lee, J.-C.; Yeo, J. K. *Macromol. Res.* **2008**, *16*, 36.
(19) Shin, J.; Bae, W.; Kim, B. G.; Lee, J.-C.; Byun, H. S.; Kim, H. *J. Supercrit. Fluids* **2008**, *47*, 1.
(20) Busch, P.; Krishnan, S.; Paik, M.; Toombes, G. E. S.; Smilgies, D. M.; Gruner, S. M.; Ober, C. K. *Macromolecules* **2007**, *40*, 81.
(21) Lee, B.; Park, Y. H.; Hwang, Y. T.; Oh, W.; Yoon, J.; Ree, M. *Nat. Mater.* **2005**, *4*, 147.
(22) Shimizu, T.; Tanaka, Y.; Kutsumizu, S.; Yano, S. *Macromolecules* **1996**, *29*, 156.
(23) *CRC Handbook of Chemistry and Physics*, 81st ed.; Lide, D. R., Ed. (section 9); CRC Press: Boca Raton, FL, 2000; p 44.
(24) Volkov, V.; Plate, N.; Takahara, A.; Kajiyama, T.; Amaya, N.; Murata, Y. *Polymer* **1992**, *33*, 1316.
(25) Lee, J.-C.; Litt, M. H.; Rogers, C. E. *Macromolecules* **1998**, *31*, 2440.
(26) Lee, J.-C.; Lim, M. Y.; Oh, K.; Lee, H. B.; Kim, Y. G.; Park, S. Y.; Farmer, B. L. *Polymer* **2002**, *43*, 7051.
(27) Stohr, J. *NEXAFS spectroscopy*; Springer series in surface sciences 25; Springer-Verlag: Berlin, 1992; p 625.
(28) Zubavichus, Y.; Shaporenko, A.; Grunze, M.; Zharnikov, M. *J. Phys. Chem. B* **2006**, *110*, 3420.
(29) Genzer, J.; Sivaniah, E.; Kramer, E. J.; Wang, J.; Xiang, M.; Char, K.; Ober, C. K.; Bubeck, R. A.; Fischer, D. A.; Graupe, M.; Colorado, R., Jr.; Shmakova, O. E.; Lee, T. R. *Macromolecules* **2000**, *33*, 6068.
(30) Luning, J.; Stohr, J.; Song, K. Y.; Hawker, C. J.; Iodice, P.; Nguyen, C. V.; Yoon, D. Y. *Macromolecules* **2001**, *34*, 1128.
(31) Krishnan, S.; Wang, N.; Ober, C. K.; Finlay, J. A.; Callow, M. E.; Callow, J. A.; Hexemer, A.; Sohn, K. E.; Kramer, E. J.; Fischer, D. A. *Biomacromolecules* **2006**, *7*, 1449.
(32) Li, X.; Andruzzi, L.; Chiellini, E.; Galli, G.; Ober, C. K.; Hexemer, A.; Kramer, E. J.; Fischer, D. A. *Macromolecules* **2002**, *35*, 8078.
(33) Busscher, H. J.; van Pelt, A. W. J.; de Boer, P.; de Jong, H. P.; Arends, J. *J. Colloids Surf.* **1984**, *9*, 319.
(34) Kwok, D. Y.; Neumann, A. W. *Adv. Colloid Interface Sci.* **1999**, *81*, 167.
(35) Martinelli, E.; Menghetti, S.; Galli, G.; Glisenti, A.; Krishnan, S.; Paik, M. Y.; Ober, C. K.; Smilgies, D.-M.; Fischer, D. A. *J. Polym. Sci.; Polym. Chem.* **2008**, *47*, 267.
(36) We also calculated critical surface energy values of polymers using hydrocarbon probe liquids. Critical surface energy values of PST−O, PST−S, and PST−SO_2 are 4.50, 3.51, and 2.49 mJ/m2, respectively. This trend is very similar with other experimental data such as tilt angle of fluorinated alkyl side chain measured by NEXAFS and distance between fluorinated alkyl side chains measured by GIWAXS.
(37) Tavana, H.; Neumann, A. W. *Adv. Colloid Interface Sci.* **2007**, *132*, 1.
(38) Youngblood, J. P.; Andruzzi, L.; Ober, C. K.; Hexemer, A.; Kramer, E. J.; Callow, J. A.; Finlay, J. A.; Callow, M. E. *Biofouling* **2003**, *19*, 91.

MA8027535